

Article

Communication and Sensing Circuits on Cellulose

Federico Alimenti *, Chiara Mariotti, Valentina Palazzi, Marco Virili, Giulia Orecchini,
Paolo Mezzanotte and Luca Roselli

Department of Engineering, University of Perugia, via G. Duranti 93, 06125 Perugia, Italy;
E-Mails: chiamariotti23@gmail.com (C.M.); palazzi.valentina.89@gmail.com (V.P.);
virili.marco@gmail.com (M.V.); giulia.orecchini@gmail.com (G.O.);
paolo.mezzanotte@unipg.it (P.M.); luca.roselli@unipg.it (L.R.)

* Author to whom correspondence should be addressed; E-Mail: federico.alimenti@unipg.it;
Tel.: +39-075-585-3642; Fax: +39-075-585-3654.

Academic Editor: Domenico Zito

Received: 31 March 2015 / Accepted: 11 June 2015 / Published: 25 June 2015

Abstract: This paper proposes a review of several circuits for communication and wireless sensing applications implemented on cellulose-based materials. These circuits have been developed during the last years exploiting the adhesive copper laminate method. Such a technique relies on a copper adhesive tape that is shaped by a photo-lithographic process and then transferred to the hosting substrate (*i.e.*, paper) by means of a sacrificial layer. The presented circuits span from UHF oscillators to a mixer working at 24 GHz and constitute an almost complete set of building blocks that can be applied to a huge variety communication apparatuses. Each circuit is validated experimentally showing performance comparable with the state-of-the-art. This paper demonstrates that circuits on cellulose are capable of operating at record frequencies and that ultra- low cost, green *i.e.*, recyclable and biodegradable) materials can be a viable solution to realize high frequency hardware for the upcoming Internet of Things (IoT) era.

Keywords: circuits on cellulose; paper-based substrates; green electronics; all-natural electronic; wireless sensors; Internet of Things (IoT)

1. Introduction

Recent United Nations estimates indicate in 50 million of metric tons the mass of electronic waste that is produced each year worldwide [1]. This number is significant (almost 9 times the mass of the Cheops pyramid) and will surely increase in the future with the development of the so-called Internet of Things (IoT), an approach which involves the use of billions of sensors distributed in the environment.

These wastes are rich in both precious materials (gold, copper, *etc.*) and highly polluting. The most dangerous parts are formed by the Printed Circuit Boards (PCB), typically made of glass fiber materials. The PCB are also treated with phenolic resins (Brominated bisphenol-A BPA epoxy resins), a substance which is very risky to release to the environment. For these reasons, the city of San Francisco, a city world-leading techniques for waste disposal, treats dismissed electronic equipments as hazardous waste.

A new way is, however, possible: the use of biodegradable and easily recyclable materials in electronics. This trend of research has emerged in the last decade and is producing a growing number of scientific studies worldwide [1–3]. Among the various possibilities, cellulose based materials (such as paper) are attracting considerable interest. Cellulose, in fact, is a natural polymer very abundant on Earth, biodegradable, available at very low cost and for which there is already an established production chain. Using these materials, a number of building blocks widely used in communication and sensing electronic hardware have already been demonstrated, among them: antennas [4], oscillators [5], accelerometers [6], RFID tags [7], energy harvesting systems [8] and devices like organic semiconductor MOS transistors [9,10].

Figure 1 illustrates the basic building blocks of three different communication systems, namely: a super-heterodyne receiver, a harmonic RFID tag and a Doppler radar sensor. The main circuits involved are: antennas, amplifiers, oscillators, mixers, power dividers, frequency multipliers, *etc.* In order to demonstrate the feasibility on cellulose of the systems in Figure 1, it is necessary to design, fabricate and experimentally validate these building blocks. Furthermore it is needed to do such a job for different operating frequencies ranging from VHF and UHF bands to microwave and millimeter-waves [11].

In this contribution, a review of circuits for communication and wireless sensing applications is proposed. These circuits are all implemented on cellulose-based materials and have been developed during the last years, exploiting the novel copper laminate method [12]. Such a technique relies on a copper adhesive tape that is shaped by a photo-lithographic process and then transferred to the hosting substrate (*i.e.*, paper) by means of a sacrificial layer. Exploiting such an approach many circuits have been built reaching a typical resolution of 150 μm line and gap widths that is suitable for distributed circuits up to millimeter-waves. In addition, the copper tracks are characterized by low losses and allow standard Surface Mount Technology (SMT) components to be soldered on the fabricated PCB.

The present article is organized as follows: Section 2 describes the used cellulose-based materials and the adhesive laminate fabrication methodology. Section 3 proposes four different building blocks on cellulose, namely an antenna, an oscillator, a mixer and a frequency doubler. For each of them the experimental results are illustrated and briefly discussed. The conclusions are finally drawn in Section 4.

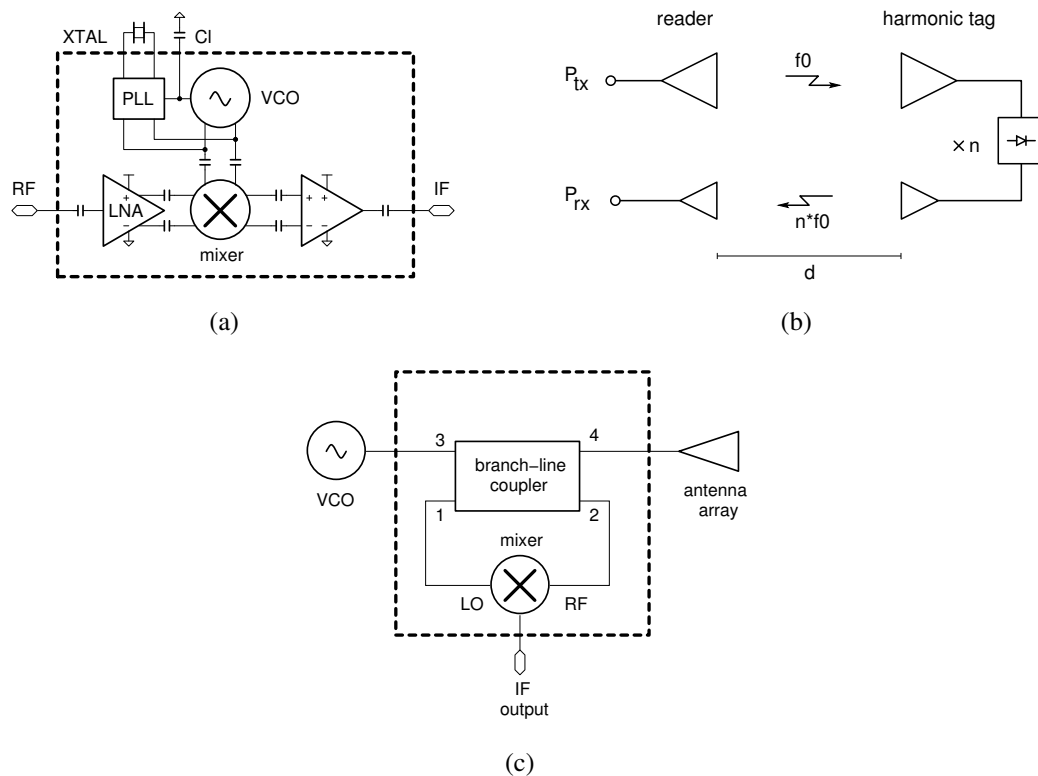


Figure 1. Architecture of three typical communication and wireless sensing systems, namely: **(a)** super-heterodyne receiver; **(b)** harmonic RFID tag; **(c)** Doppler radar sensor. The main building blocks involved are antennas, amplifiers, oscillators, mixers and frequency multipliers.

2. Materials and Method

The basic idea of this paper is to systematically investigate the performance and the main design challenges of microwave circuits implemented on cellulose-based materials. For this reason it is convenient to start from the material itself. After several tests the Mitsubishi-Electric (TM) photographic paper has been selected as a suitable dielectric material for the substrate. The features of cellulose-based substrates that are mostly attractive in electronics are low cost and low environmental impact. Cellulose, indeed, is the most common natural polymer and it is widespread employed: from the paper of journals and books to the cardboard of packaging and, in the last years, to the amazing mechanical structures conceived by the architect Shigeru Ban [13]. Among the properties of paper-based materials, it is interesting to report the capability to be folded and conformed to curved objects, which can be of some importance in the circuit design. Finally, one should consider that the technologies to produce and manufacture cellulose composites are mature and constitute a solid background for new applications.

To substitute standard PCBs with cellulose-based ones, a good conductor to implement the metal tracks is needed. In this study the metal tracks are realized exploiting an adhesive copper laminate from Advance (TM). It is worth noticing here that, such a laminate, comes with an idrofobic acrylic adhesive that behaves like a good dielectric material. The principal electrical parameters of these materials (cellulose-based substrate and copper laminate) are quoted in Table 1. The roughness of the Mithsubishi

Electric photo-paper (glossy side) has been measured with an Atomic Force Microscope (AFM) and is around 0.05 μm . This value is negligible for the considered applications.

Table 1. Material Characteristics.

Parameter	Substrate	Laminate
company	Mitsubishi-Electric (TM)	Advance (TM)
material	cellulose-based	copper
thickness	230 μm	35 μm
		(copper)
		30 μm
		(adhesive)
ϵ_r	3.2	1.3
	(paper)	(adhesive)
$\tan \delta$	0.08	n.a.
σ	n.a.	$5.8 \times 10^7 \text{ S/m}$

The third element needed to fabricate the PCB is a method to shape the metal tracks and to transfer them to the substrate. Among several approaches like ink-jet printing and screen printing (both with conductive inks), the copper laminate method is adopted here, [12]. It is composed of five steps. In the first step, a photo-resist film is deposited on the copper laminate surface and the circuit layout is transferred to it exploiting a mask, a UV light source and a developer, see Figure 2a. In the second step, the copper is etched, see Figure 2b. Such a step exposes the adhesive layer where the copper has been removed whereas, on the opposite side, it remains covered by the protection layer of the adhesive laminate tape (P in the figure). In the third step, a sacrificial layer is attached on the copper side and the protection layer is removed, see Figure 2c. The sacrificial layer has a very important function, that is to keep unaltered during the transfer process the relative distances among the layout features, even when these are not physically connected. In the fourth step, the etched metal is transferred to the hosting cellulose-based substrate as in Figure 2d and, finally, the sacrificial layer is removed, Figure 2e. This last step also removes the exposed adhesive material.

To test the above fabrication method a 30 mm long microstrip line is etched and transferred to the paper substrate. The ground-plane is realized with another piece of copper laminate attached to the bottom side of the substrate. The microstrip is designed to have a characteristic impedance of 50 Ω and thus has a width of about 0.9 mm. Figure 3 reports the measurement of the transmission parameter S_{21} up to 10 GHz, showing a magnitude of -1.8 dB (*i.e.*, about 0.8 dB/cm of overall losses). From the same graph it can be seen that the fabricated microstrip is better than a similar structure implemented with an ink-jet printing process. This result is due to the superior conductivity of the bulk copper laminate with respect to the cured Ag ink. The study [12] was very important since it established the right materials and the right methods for microwave circuits on cellulose.

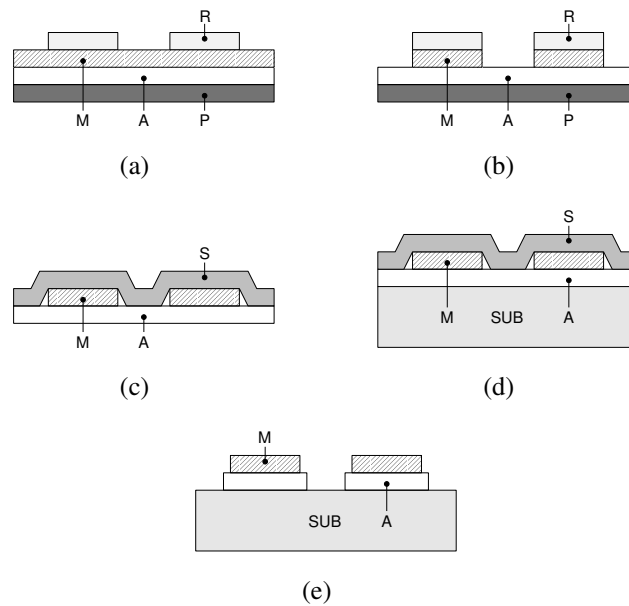


Figure 2. Process steps for the circuit fabrication. In (a) the photo-resist is deposited on the conductive laminate and patterned using UV and a developer. Then, the conductive layer is etched. This exposes the adhesive layer underneath (b). Finally, in (c–e), the conductor is transferred on the cellulose substrate by means of a sacrificial layer. M: metal, A: adhesive, P: protection, R: photo-resist, S: sacrificial layer, SUB: hosting substrate. Reproduced with permission from [12]. Copyright 2012, IEEE.

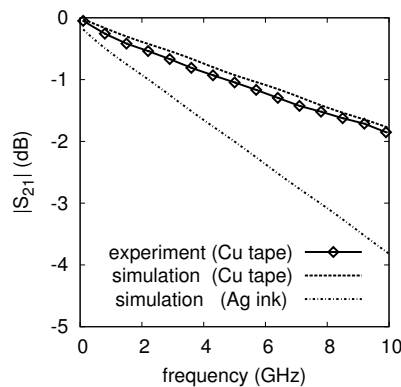


Figure 3. Transmission parameter S_{21} of a 50 Ω , copper microstrip line versus the frequency. The track is 30 mm long and is compared with a similar structure made out of Ag ink (3 μm ink thickness, $\sigma_{ink} = 1.1 \times 10^7$ S/m after curing). Reproduced with permission from [12]. Copyright 2012, IEEE.

3. Results and Discussion

In this section several microwave circuits on cellulose are presented and briefly discussed. These circuits constitute an almost complete set of building blocks that can be applied to communication apparatus, wireless sensors and, more in general, to any RF hardware.

3.1. Antennas

In communication hardware, antennas play a fundamental role because they capture or radiate the electromagnetic waves. In receivers, the captured waves are transduced into oscillating voltage and current that are sent toward the input of the receiver itself. In transmitters, on the contrary, the oscillating voltage and current available at its output are converted into waves by the antenna and radiated in the surrounding space. To do such a job an antenna should have a physical dimension comparable to that of the wavelength, $\lambda_0 = c/f_0$ where c is the light speed in the considered media and f_0 is the carrier frequency. This means that antennas cannot be miniaturized below a certain limit, typically between $\lambda_0/8$ and $\lambda_0/4$ for an elementary radiating element. In other words, while electronic has followed the Moore's law during the last five decades, antennas have not because, physically, they cannot. As a consequence the mass of material needed to fabricate an antenna can be significant if compared to that of a wireless gadget, particularly when highly miniaturized single-chip or System-on-Chip (SoC) transceivers are employed. For this reason antennas have been the first RF building block to be designed and tested on cellulose substrates [4,14]. Furthermore, paper antennas will be more and more important in the IoT era when both the cost per unit and the environmental impact of dismissed apparatuses will be of paramount importance.

As an example, a planar patch antenna and a 2×2 patch antenna array are considered as cases-of-study in the present contribution. Both these structures are implemented on cellulose exploiting the materials and the method described in Section 2 and they operate at 24 GHz. Such a frequency is very high and has been selected to make an extreme test of both technology and material performance. To the best author's knowledge this is a record frequency for paper antennas, at least until the year 2014.

First a single patch (radiating element) has been designed, fabricated and validated, see Figure 4a. Such a patch has a square shape with a side of 3.9 mm, *i.e.*, close to half a wavelength in the material at the operating frequency. A quarter wave impedance transformer is used in this case to match the quite high input impedance of the patch to the 50Ω level of the feeding microstrip.

After verification, the single patch has been used as radiating element in a 2×2 patch array antenna, see Figure 4b. The purpose of the array is to have a broadside radiation and to improve the gain with respect to that of the simple patch. In order to avoid grating lobes in the visible region, the spacing between the array elements is kept below $\lambda_0/2$. A particular characteristic of such a design is that the structure uses three metal layers, a top layer where the patches are placed, a central layer exploited as common ground plane and a third layer (not visible in the picture) where the feeding line is fabricated.

The feeding network of the antenna array is formed by three power dividers. The first two are implemented in the same metal layer as the radiating elements (T-junctions), while the third one is constituted by the via-trough wire connecting the antenna to the bottom feeding line. The experiments show a gain of about 7.4 dBi with a radiation efficiency of 35%. The half power beam-widths are 55° in the E-plane cut and 48° in the H-plane cut. The input reflection coefficient is equal to -29 dB at the center frequency and remains below -20 dB in a 540 MHz bandwidth.

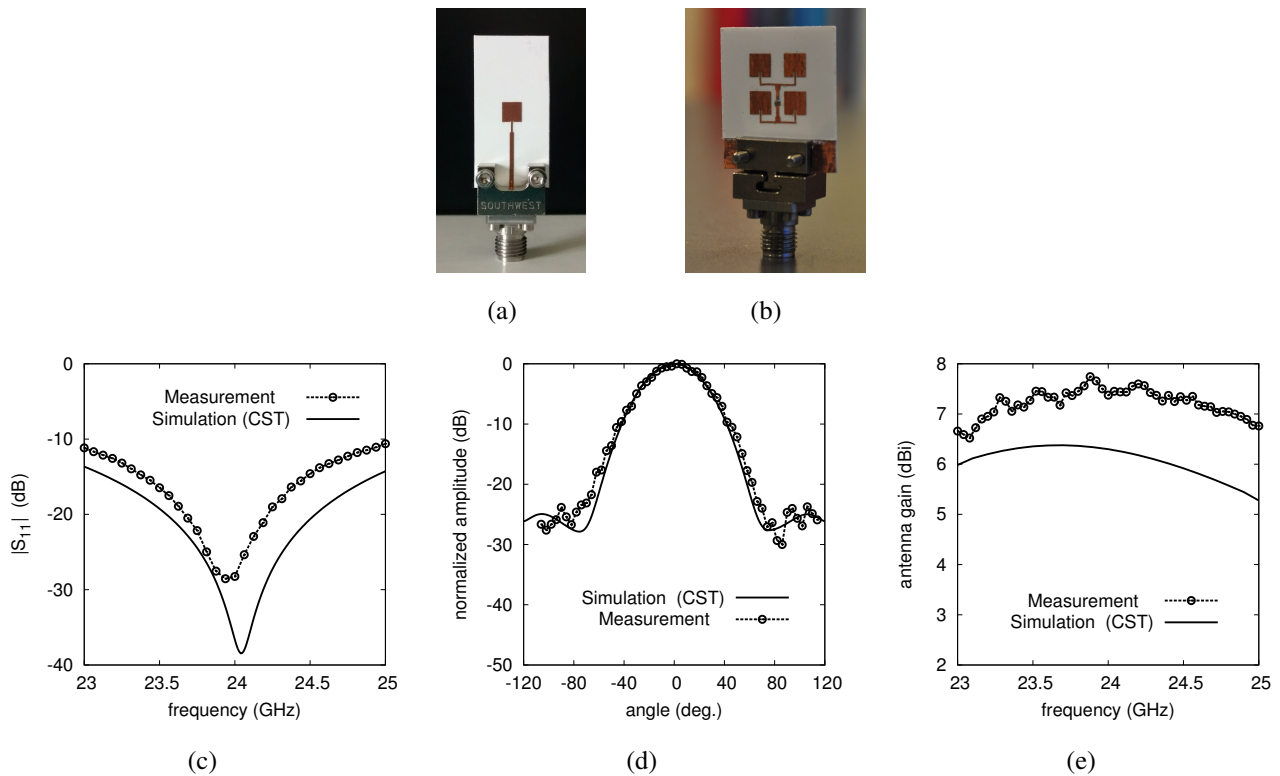


Figure 4. Fabricated 24 GHz single patch antenna (a) and patch antennas array (b). The 2×2 array is measured and compared with electromagnetic simulations, namely: input reflection coefficient (c), H-plane radiation pattern (d) and radiation gain (e). The half-power beam width is about 48° whereas the radiation gain is 7.4 dBi at center frequency. Reproduced with permission from [15]. Copyright 2014, Institution of Engineering & Technology (IET).

3.2. Oscillators

Oscillators are pervasive circuits that can be used to transmit RF signals, to convert their frequency (in conjunction with mixers) or to send identification information (RFID). For these reasons they are one of the most important building blocks of a communication system hardware. Up to now only very few UHF oscillators based on paper substrates have been reported in the literature, see for example ref. [5]. The last circuit, exploits the active antenna concept and its wiring network is fabricated by means of ink-jet printing with silver (Ag) nano-particles conductive ink. It uses eight lumped components (including the transistor) that are glued with a conductive epoxy on the substrate.

The differential oscillator circuit of Figure 5, instead, is aimed at minimizing the number of components. This issue is of great importance in the development of disposable wireless sensors for IoT applications since it directly affect the production cost. It uses a cross-coupled BJT pair as negative resistor and, for the first time, a distributed hairpin resonator and a proximity output coupler both implemented on a cellulose-based substrate.

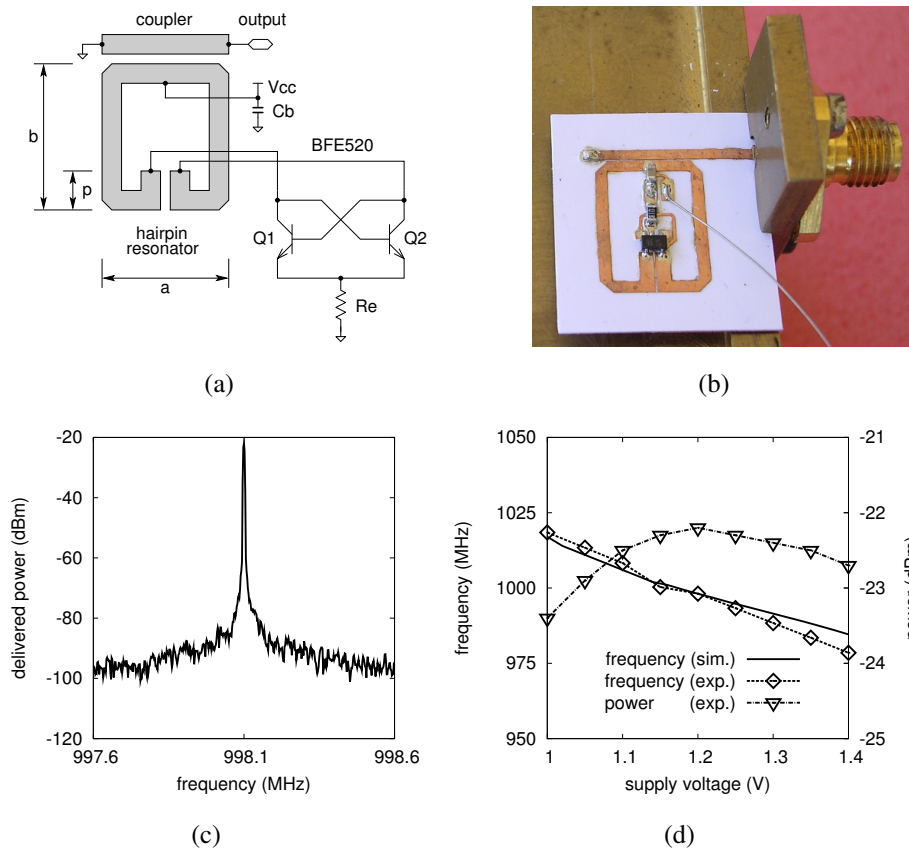


Figure 5. Fabricated 1.2 V, 0.75 mA UHF oscillator. Circuit schematic (a); fabricated prototype (b); output spectrum (c) and tuning characteristic (d). The oscillator uses a hairpin microstrip (distributed) resonator and a cross-coupled BJT pair. It operates at 998 MHz and has a size of $a = 9.8$ mm in width and $b = 11$ mm in height. Reproduced with permission from [16]. Copyright 2013, IEEE.

From the analysis of Figure 5a one can notice that the base of Q1 is DC connected to the collector of Q2 and vice-versa. Although this solution is not optimal from the performance point of view, it allows to simplify the circuit. With the collector to base DC connection, indeed, the BJTs enter in saturation for relatively low oscillation amplitudes [17] (p. 98). Such a behavior, however, is not a problem if a relatively low output power is required, a condition that happens in short-range wireless links.

The hairpin resonator is designed following the guidelines reported in [18] and considering the capacitive loading due to the differential transistor pair. The resonator is modeled by means of equivalent circuits under ADS of Keysight Technology. At the operating frequency it features a quality factor of about 70. The oscillator has been optimized for low-power consumption exploiting the Harmonic Balance (HB) solver. The circuit prototype is shown in Figure 5b and has been implemented again with the materials and methods illustrated previously.

Only three external components are needed, namely: the single-package BFE520 BJT pair, the resistor $R_e = 1$ k Ω and the bypass capacitor $C_b = 1$ nF. These devices are soldered on the cellulose-based circuit by setting the iron tip temperature to 250 °C, this in order to preserve the substrate. The measured output spectrum is reported in Figure 5c. At 1.2 V the oscillator draws a DC current of 0.75 mA with a 0.9 mW power consumption. The output frequency is about 998 MHz whereas it delivers a power of -22 dBm to

a $50\ \Omega$ load. The corresponding phase noise is $-99\ \text{dBc/Hz}$ at $100\ \text{kHz}$ frequency offset from the carrier. These results compares well with the present state-of-the-art for low-power UHF oscillators.

The designed circuit can act as a VCO by varying its supply voltage. This means that the modulation signal must be superimposed to V_{cc} . Such a solution, *i.e.*, not having a separate tuning port, popular with Gunn oscillators, [19], is selected here to minimize the circuit complexity. Figure 5d illustrates the results of a frequency tuning experiment. The output frequency can be varied from $1018\ \text{MHz}$ to $978\ \text{MHz}$ when the voltage goes from $1\ \text{V}$ to $1.4\ \text{V}$. The tuning sensitivity is about $-100\ \text{MHz/V}$, and the output power is almost constant. As the supply voltage increases the output frequency decreases due to the diffusion capacitance of the BE junctions. This capacitance, indeed, is proportional to I_C^0 , and thus to V_{cc} , according to: $\tau_F I_C^0 / V_T$, τ_F being the forward transit time and V_T the thermal voltage. The temperature stability of the oscillation frequency is about $-290\ \text{ppm/}^\circ\text{C}$.

3.3. Mixers

The mixer is another key building block in communication hardware and microwave sensors. This circuit, indeed, is used to perform the frequency conversion, a basic function in super-heterodyne architectures. Moreover, in Doppler radars, the mixer allows for the detection of the small frequency difference between transmitted and received signals. To the best of the authors' knowledge, microwave mixers on paper substrate have never been published before the year 2013.

The $24\ \text{GHz}$ mixer shown in Figure 6a is intended for zero- or low-IF operation; it exploits a single-balanced architecture and uses a 180° hybrid junction (rat-race) in microstrip technology. This configuration features good performances in terms of both conversion losses and RF/LO isolation. Furthermore it requires a minimum number of discrete components.

The diodes D1 and D2 are placed inside the ring to save space and the microwave signal is shorted at one side of them by using radial stubs. The IF signal is picked-up by a jumper (implemented with a $0\ \Omega$ resistor) and routed outside the ring. A third radial stub is used here to provide a further isolation between IF and RF/LO ports. The DC return for the diodes is realized by a quarter wave short-circuited stub, G in Figure 6a. The two stubs on the RF/LO input lines are used to improve the impedance matching of these ports. The diodes adopted in the mixer are two low-barrier Si Schottky devices from MA-COM [21]; their SPICE model is reported in [22]. The ring has a perimeter $l_h = 3\lambda/2$ and a characteristic impedance of $70.7\ \Omega$. A Harmonic Balance (HB) simulator is adopted to perform the mixer design. RF and LO ports are matched to $50\ \Omega$. The IF resistance R_{IF} is equal to $240\ \Omega$, a value optimized for the minimum conversion loss.

The circuit is realized on the Mitsubishi Electric photo-paper substrate with copper adhesive laminate process. The external diameter of the rat-race ring is $4.6\ \text{mm}$ while the diodes are only 1-mm long; two values testifying the accuracy that can be achieved with the proposed fabrication methodology.

For the mixer characterization two $50\ \Omega$ microwave sources are used to provide the RF and LO signals. The IF power, instead, has been measured on a $240\ \Omega$ termination, using the asymmetrical attenuator described in [22] and a spectrum analyzer. The measured conversion loss of the mixer is reported in Figure 6c and reaches $10\ \text{dB}$ at the optimum driving level of $2.3\ \text{dBm}$. For a LO power less than $-7\ \text{dBm}$ the experimental curve saturates. This is due to the noise limits of the spectrum analyzer used to measure

the IF power. Figure 6d shows the mixer conversion loss versus the LO frequency. The mixer is well centered around 24 GHz and features a bandwidth of about ± 150 MHz, which is suitable for zero-IF applications. The simulated 1 dB compression point and third-order input intercept point are 0 dBm and +11 dBm respectively. These results compare well with the state-of-the-art for 24 GHz diode mixers implemented with standard technologies (typical conversion loss of 7 dB).

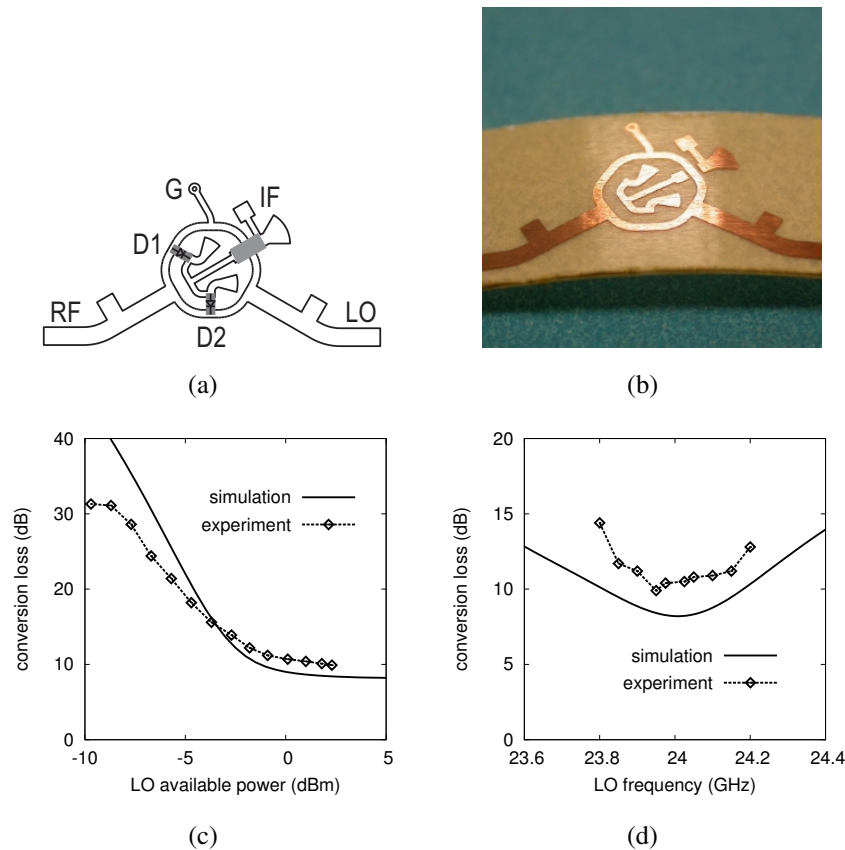


Figure 6. Fabricated 24 GHz Schottky diode mixer. Circuit schematic (a); fabricated layout (b); conversion loss versus local oscillator power (c) and frequency (d). In (c) the available LO power is swept while $f_{RF} = 24$ GHz, $f_{LO} = 23.95$ GHz and $f_{IF} = 50$ MHz. In (d) the available LO power is $P_{LO} = 2.3$ dBm (optimum driving level), $f_{RF} = 24.06$ GHz and the LO frequency is varied. In both (c) and (d) $P_{RF} = -30$ dBm. Reproduced with permission from [20]. Copyright 2013, IEEE.

3.4. Frequency Doublers

Frequency doublers are used in transmitters or receivers when twice the frequency of the local oscillator is needed. They also find application in harmonic RFID systems like those described in [23,24]. In RFID applications they should feature a low conversion loss, even at low input power, with a minimum component count and PCB area [25]. The cellulose frequency doubler schematic is shown in Figure 7a. A HSMS-2850 Schottky diode from Keysight [26] is adopted to perform the frequency multiplication, by the non-linearity of its I-V characteristic.

The circuit works as follows: the diode distorts the input waveform at the fundamental frequency f_0 . Such a distortion generates harmonics and the two $\lambda/4$ stubs (at f_0), placed on both sides of the diode, select the proper frequency component. The short-circuit stub at the input side, l_s in Figure 7a allows the f_0 tone to reach the diode, whereas it reflects the second harmonic $2f_0$ toward the output. On the other hand, the open-circuit stub at the output side, l_o in Figure 7a, short-circuits the f_0 component without affecting the $2f_0$ signal (*i.e.*, is an open circuit for it). This happens because, at $2f_0$, the above stubs are half wave long. Stubs isolates input and output from each other facilitating the design of matching circuits on both sides.

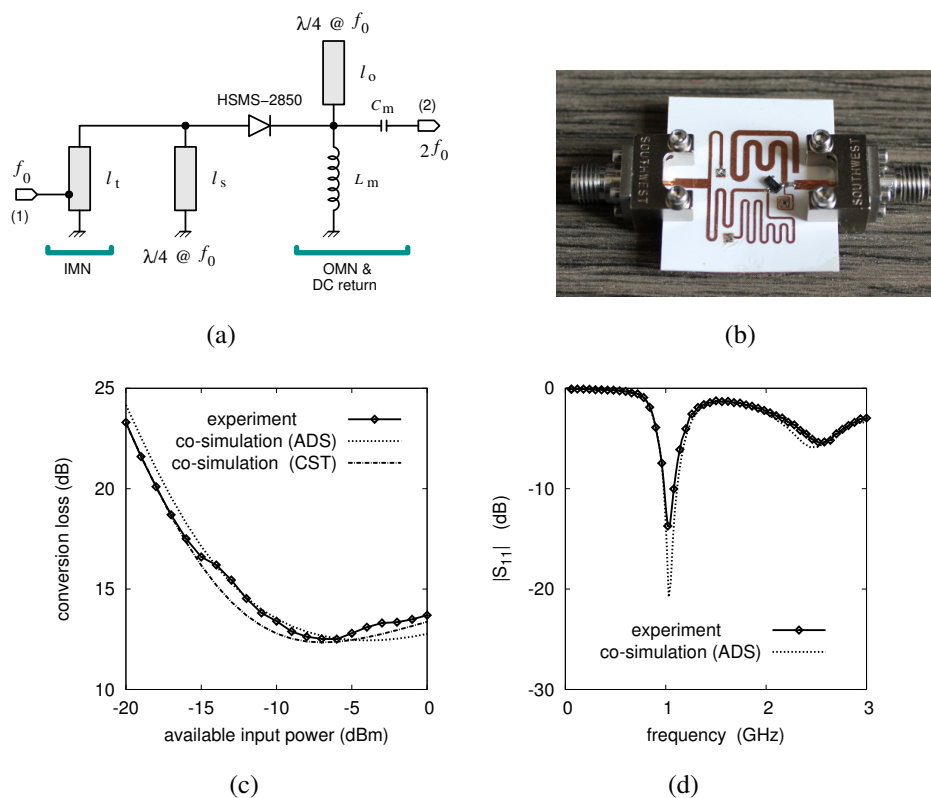


Figure 7. Fabricated low-power, Schottky diode frequency doubler. Circuit schematic (a); fabricated prototype (b); conversion loss versus input power (c) and input reflection coefficient (d). For an input signal at 1.04 GHz with a -10 dBm level the measured conversion loss is 13.4 dB with a reflection coefficient of -14 dB. Active area: 18 mm in length and 19 mm in width. Reproduced with permission from [27]. Copyright 2014, IEEE.

The Input Matching Network (IMN) consists of a tapped impedance transformer, the purpose of which is to increase the 50Ω source impedance to the conjugate, large-signal input impedance of the diode. This is about 266Ω in magnitude for a 0.1 mW available input power. The tapped transformer can be easily implemented with the adopted fabrication method (no external components needed) and it is superior to L-type lumped networks, especially for high impedance ratios. The Output Matching Network (OMN), instead, is used to transform the 50Ω (output) port impedance in the optimum load impedance Z_l^o that gives the minimum conversion loss for the diode. This value is $Z_l^o = 160 + j80 \Omega$ and has been found with Harmonic-Balance (HB) simulations. The OMN is realized in the form of a LC network: L_m and C_m in Figure 7a. Note that, in the layout of Figure 7b, L_m is printed and also acts as

a DC return for the diode. As a result, the only external components needed by this circuit are, thus, the diode and the capacitor C_m .

To validate the frequency doubler, its layout is fabricated and transferred from the Cu laminate to the photo-paper via the sacrificial layer, see Figure 7b. A sheet of adhesive Cu is attached to the bottom side of the substrate to realize the microstrip ground plane. The via-hole contacts are implemented by wire soldering. The experiments are reported in the bottom panels of Figure 7. In particular, Figure 7c represents the conversion loss as a function of the available power of the input source, whereas Figure 7d depicts the input reflection coefficient $|S_{11}|$ versus the frequency. For an input power of -10 dBm a minimum conversion loss of 13.4 dB is measured. The magnitude of $|S_{11}|$, instead, is -14 dB at the operating frequency of 1.04 GHz. The overall agreement between experiments and simulations is good.

4. Conclusions

In this work, for the first time, an almost complete set of circuits on cellulose for communication and sensing applications is illustrated. These circuits are implemented through the copper laminate approach, a technique characterized by low conductor loss and compatible with the soldering process of surface-mount electronic components. Record frequencies are demonstrated by a mixer and by an antenna working at 24 GHz, *i.e.*, at the boundary between microwaves and millimeter waves. At lower frequencies a low-power UHF oscillator and a Schottky diode frequency doubler have been developed for RFID and sensing applications. In all the presented cases the circuits are verified experimentally, showing performance that are comparable to the present state-of-the-art. A preliminary cost analysis shows that a low series production can be kept below 0.01 \$ per square centimeter and that such a price can be significantly lowered for mass production. In conclusion the presented study indicates a viable solution for the realization of high frequency hardware that is simultaneously ultra low-cost, green (*i.e.*, recyclable and biodegradable) and, for these reasons, suitable for the future Internet of Things (IoT) distributed electronics.

Acknowledgments

The authors are grateful to Keysight Technologies and Computer Simulation Technologies for the donation of the ADS and CST software licenses respectively. This work was supported in part by the following research projects: ARTEMOS, Agile RF Transceiver and Front-Ends for Future Smart Multi-Standard Communications Applications (ENIAC-MIUR, call 3, 2010); ENLIGHT, Energy Efficient and Intelligent Lighting Systems (ENIAC-MIUR, call 3, 2010); GRETA, Green Tags and Sensors with Ultrawideband Identification and Localization Capabilities (MIUR, 2011).

Author Contributions

The research is shared in equal part among the authors. Federico Alimenti has edited the manuscript.

Conflicts of Interest

The authors declare that part of the material presented in this paper was already published in IEEE and IET journals. All the previously published material has been rigorously referred.

References

1. Savage, N. All-natural electronics. *IEEE Spectr.* **2015**, *52*, 18.
2. Steckl, A.J. Circuits on Cellulose. *IEEE Spectr.* **2013**, *50*, 48–61.
3. Yang, L.; Rida, A.; Vyas, R.; Tentzeris, M.M. RFID Tag and RF Structures on a Paper Substrate Using Inkjet-Printing Technology. *IEEE Trans. Microw. Theory Tech.* **2007**, *55*, 2894–2901.
4. Shaker, G.; Safavi-Naeini, S.; Sangary, N.; Tentzeris, M.M. Inkjet Printing of Ultrawideband (UWB) Antennas on Paper-Based Substrates. *IEEE Antennas Wirel. Propag. Lett.* **2011**, *10*, 111–114.
5. Kim, S.; Georgiadis, A.; Collado, A.; Tentzeris, M. An Inkjet-Printed Solar-Powered Wireless Beacon on Paper for Identification and Wireless Power Transmission Applications. *IEEE Trans. Microw. Theory Tech.* **2012**, *60*, 4178–4186.
6. Liu, X.; Mwangi, M.; Li, X.; O'Brien, M.; Whitesides, G. Paper-Based Piezoresistive MEMS Sensors. *Lab Chip* **2011**, *11*, 2189–2196.
7. Roselli, L. *Green RFID System*; Cambridge University Press: Cambridge, UK, 2014.
8. Roselli, L.; Carvalho, N.B.; Alimenti, F.; Mezzanotte, P.; Orecchini, G.; Virili, M.; Mariotti, C.; Goncalves, R.; Pinho, P. Smart Surfaces: Large Area Electronics Systems for Internet of Things Enabled by Energy Harvesting. *IEEE Proc.* **2014**, *102*, 1723–1746.
9. Fortunato, E.; Correia, N.; Barquinha, P.; Pereira, L.; Goncalves, G.; Martins, R. High-Performance Flexible Hybrid Field-Effect Transistors Based on Cellulose Fiber Paper. *IEEE Electron Device Lett.* **2008**, *29*, 988–990.
10. Valentini, L.; Cardinali, M.; Grkovic, M.; Uskokovic, P.S.; Alimenti, F.; Roselli, L.; Kenny, J.M. Flexible Transistors Exploiting P3HT on Paper Substrate and Graphene Oxide Film as Gate Dielectric: Proof of Concept. *Sci. Adv. Mater.* **2013**, *5*, 530–533.
11. Rappaport, T.S.; Roh, W.; Cheun, K. Mobile's Millimeter-Wave Makeover. *IEEE Spectr.* **2014**, *49*, 35–58.
12. Alimenti, F.; Mezzanotte, P.; Dionigi, M.; Virili, M.; Roselli, L. Microwave Circuits in Paper Substrates Exploiting Conductive Adhesive Tapes. *IEEE Microw. Wirel. Compon. Lett.* **2012**, *22*, 660–662.
13. Ban, S. Available online: <http://www.shigerubanarchitects.com/works.html> (accessed on 15 June 2015).
14. Orecchini, G.; Palazzari, V.; Rida, A.; Alimenti, F.; Tentzeris, M.M.; Roselli, L. Design and Fabrication of Ultra-Low Cost Radio Frequency Identification Antennas and Tags Exploiting Paper Substrates and Inkjet Printing Technology. *IET Microw. Antennas Propag.* **2011**, *5*, 993–1001.

15. Poggiani, M.; Alimenti, F.; Mezzanotte, P.; Virili, M.; Mariotti, C.; Orecchini, G.; Roselli, L. 24-GHz Patch Antenna Array on Cellulose-Based Materials for Green Wireless Internet Applications. *IET Sci. Meas. Technol.* **2014**, *8*, 342–349
16. Alimenti, F.; Mariotti, C.; Mezzanotte, P.; Dionigi, M.; Virili, M.; Roselli, L. A 1.2 V, 0.9 mW UHF VCO Based on Hairpin Resonator in Paper Substrate and Cu Adhesive Tape. *IEEE Microw. Wirel. Compon. Lett.* **2013**, *23*, 214–216.
17. Lacaita, A.; Levantino, S.; Samori, C. *Integrated Frequency Synthesizers for Wireless Systems*; Cambridge University Press: Cambridge, UK, 2007.
18. Yabuki, H.; Sagawa, M.; Makimoto, M. Voltage Controlled Push-Push Oscillators using Miniaturized Hairpin Resonators. In Proceedings of the IEEE MTT-S International Microwave Symposium Digest, Boston, MA, USA, 10–14 July 1991; pp. 1175–1178.
19. Chang, Y.W. Millimeter-wave (W-Band) Quartz Image Guide Gunn Oscillator. *IEEE Trans. Microw. Theory Tech.* **1983**, *31*, 194–199.
20. Alimenti, F.; Mezzanotte, P.; Giacomucci, S.; Dionigi, M.; Mariotti, C.; Virili, M.; Roselli, L. 24-GHz Single-Balanced Diode Mixer Exploiting Cellulose-Based Materials. *IEEE Microw. Wirel. Compon. Lett.* **2013**, *23*, 596–598.
21. MA/COM. *MA4E2502L - Low Barrier Silicon Schottky Diodes*. Available online: <http://www.macom.com/products/product-detail/MA4E2502L-1246> (accessed on 15 June 2015).
22. Alimenti, F.; Mezzanotte, P.; Tasselli, G.; Battistini, A.; Palazzari, V.; Roselli, L. Development of Low-Cost 24-GHz Circuits Exploiting System-in-Package SiP Approach and Commercial PCB Technology. *IEEE Trans. Compon. Packag. Manuf. Technol.* **2012**, *2*, 1265–1274.
23. Song, J.; Viikari, V.; Pesonen, N.; Marttila, I.; Seppa, H. Optimization of Wireless Sensors Based on Intermodulation Communication. *IEEE Trans. Microw. Theory Tech.* **2013**, *61*, 3446–3452.
24. Alimenti, F.; Roselli, L. Theory of Zero-Power RFID Sensors Based on Harmonic Generation and Orthogonally Polarized Antennas. *Prog. Electromagn. Res.* **2013**, *134*, 337–357.
25. Presas, S. Microwave Frequency Doubler Integrated with Miniaturized Planar Antennas. Master's Thesis, University of South Florida, Tampa, FL, USA, 2008.
26. Agilent Technologies. *HSMS-2850 Series - Surface Mount Zero Bias Schottky Detector Diodes*; Agilent Technologies: Santa Clara, CA, USA, 1999.
27. Palazzi, V.; Alimenti, F.; Mezzanotte, P.; Mariotti, M.V.C.; Orecchini, G.; Roselli, L. Low-Power Frequency Doubler in Cellulose-Based Materials for Harmonic RFID Applications. *IEEE Microw. Wirel. Compon. Lett.* **2014**, *24*, 896–898.